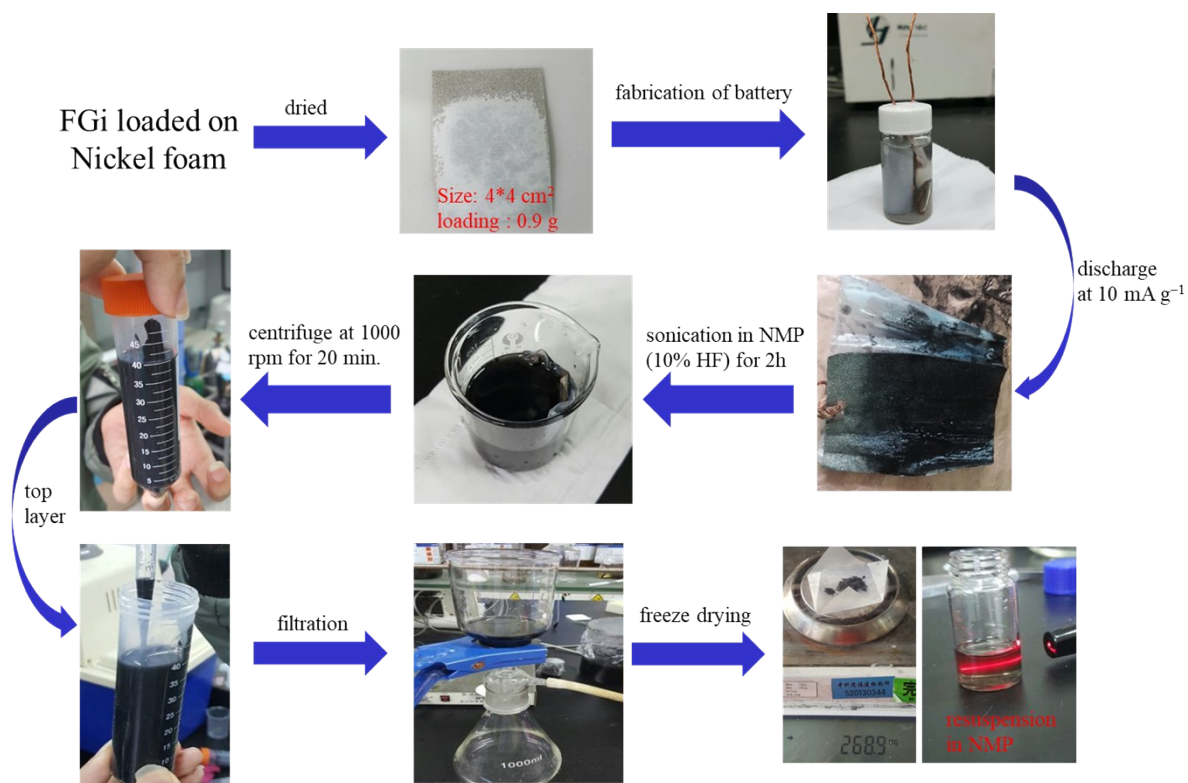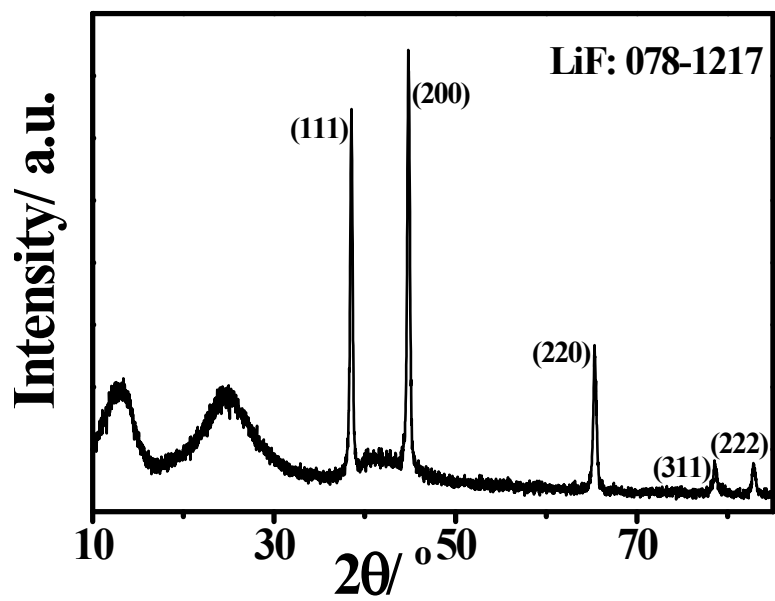# Electrochemically Scalable Production of Bilayer Fluorographene Nanosheets for Solid-State Supercapacitors

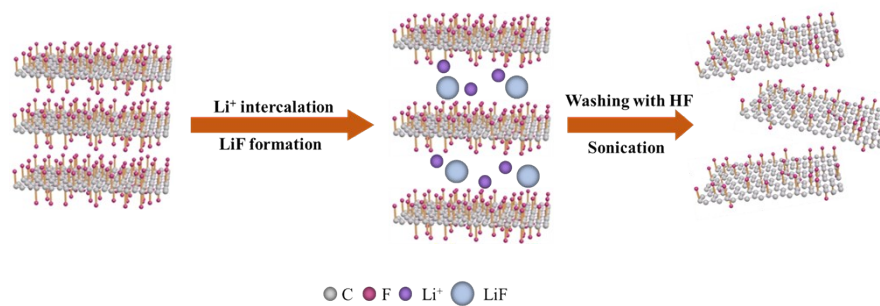Jiangquan Lv‡, Peng Zeng‡, Syed Comail Abbas, Xiangfeng Guan, Peihui Luo, Dagui Chen and Yaobing Wang*
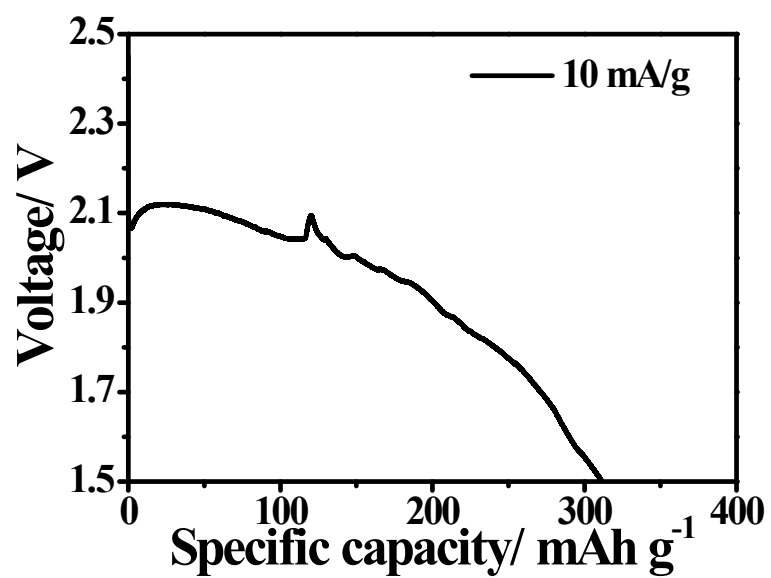
Figure S1. The whole procedures for preparation of bilayer FG nanosheets.
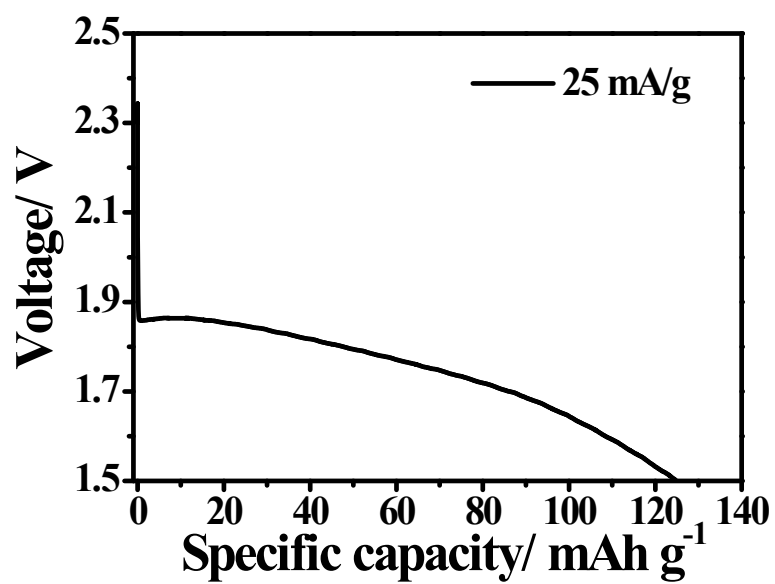
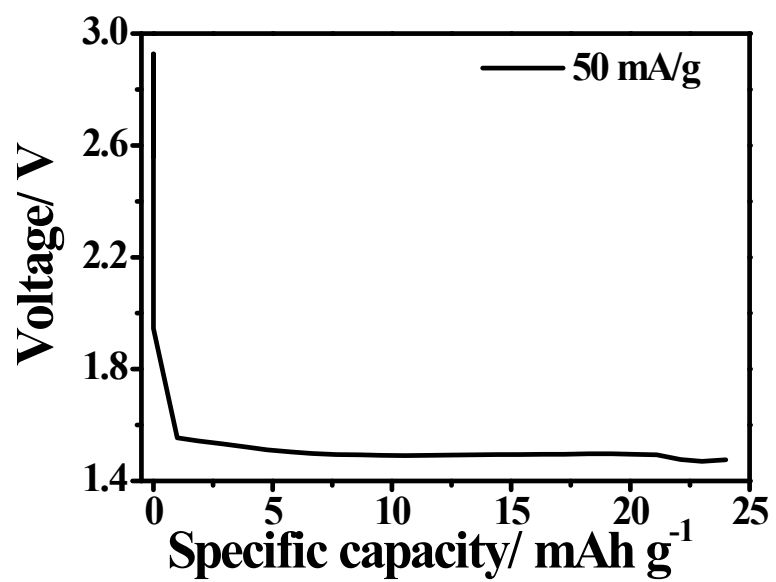**Figure S2.** The XRD pattern of discharging product without HF washing.
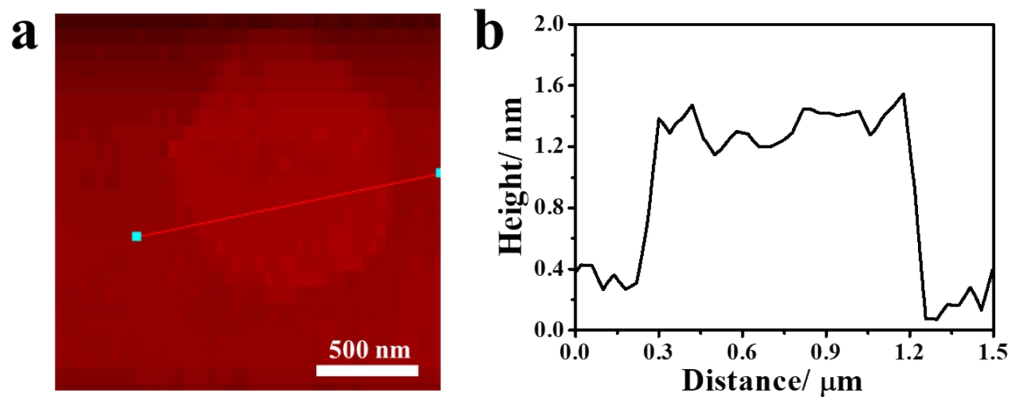
Figure S3. The detailed exfoliation mechanism.

Figure S4. The discharging curve of the Li-ion battery with FGi electrode at 10 mA g⁻¹.
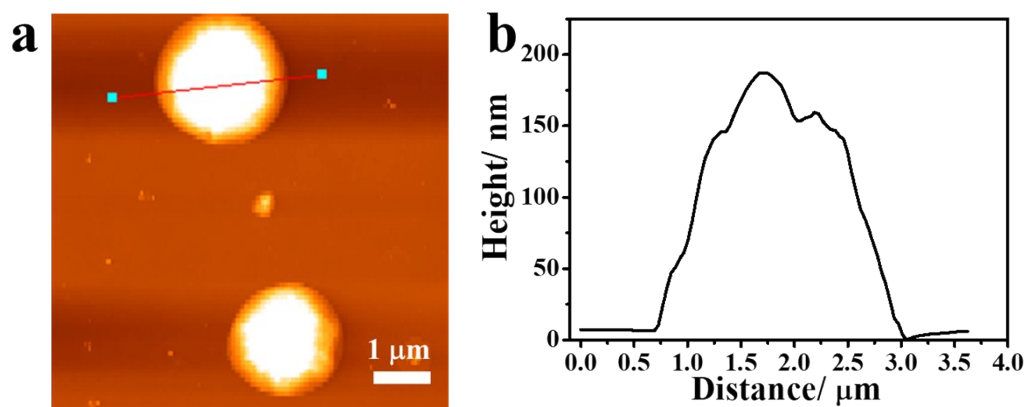
Figure S5. The discharging curve of the Li-ion battery with FGi electrode at 25 mA g^{-1}.

Figure S6. The discharging curve of the Li-ion battery with FGi electrode at 50 mA g^{-1}.

Figure S7. (a) Representative AFM image of FG nanosheet at current density of 25 mA g^{-1} and (b) the corresponding thickness analysis taken around the red line in (a).
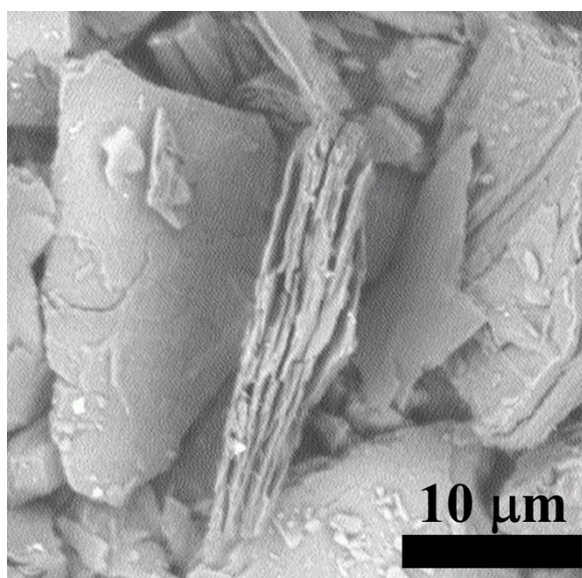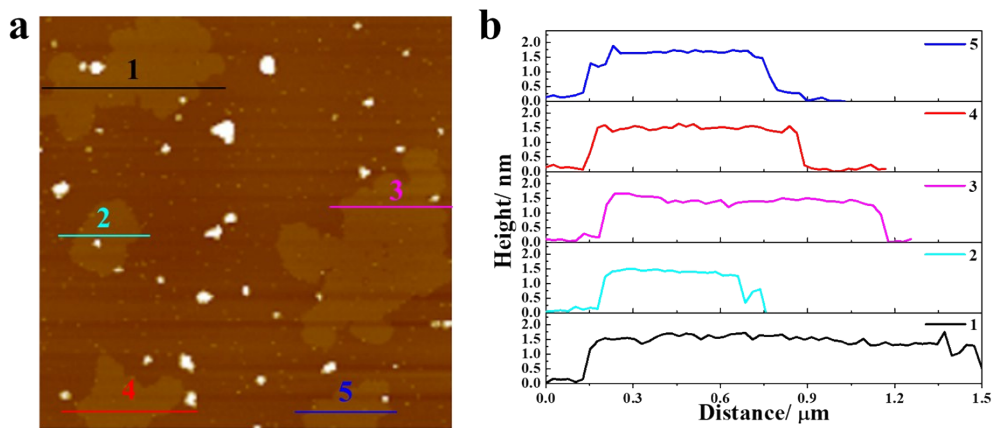
Figure S8. (a) Representative AFM image of FG nanosheet at current density of 50 mA g^{-1} and (b) the corresponding thickness analysis taken around the red line in (a).

Figure S9. The optical image of FGi loading on nickel foam (left: 8 cm × 6 cm, right: 4 cm × 4 cm).

Figure S10. The SEM image of pristine FGi.

Figure S11. (a) AFM image of FG nanosheets and (b) the corresponding thickness analysis taken around the lines in (a). We can see that almost all the FG nanosheets were the same thickness (1.5 nm, bilayer).
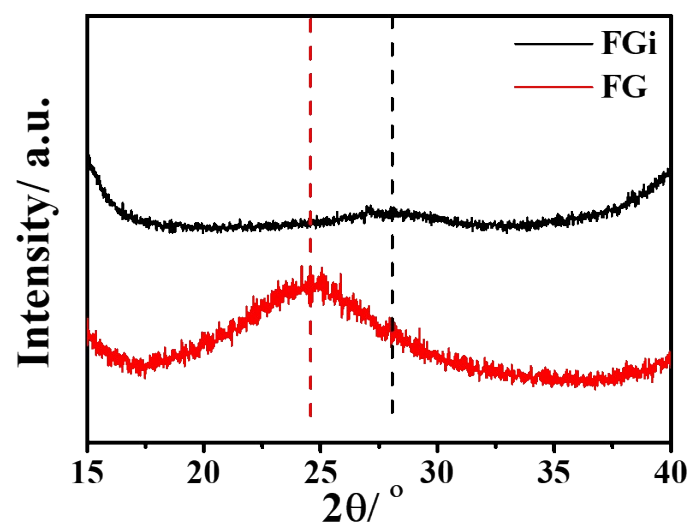
Figure S12. The enlarged XRD figure to better show the shift of (002) peak in bilayer FG nanosheets and FGi.
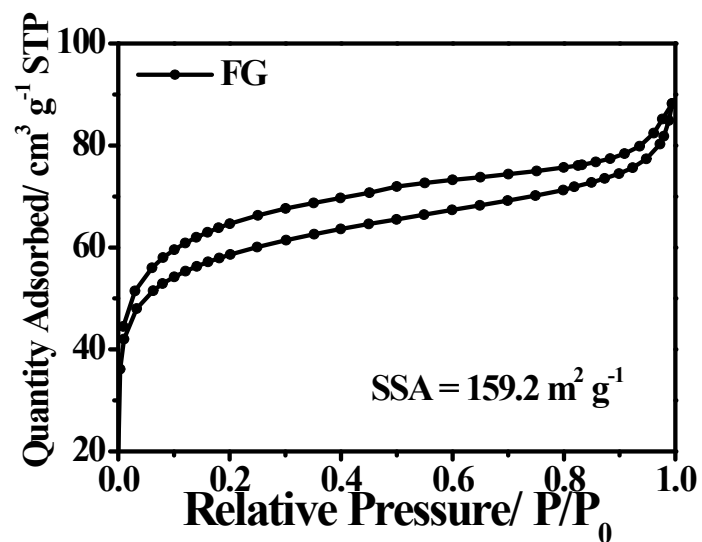
Figure S13. N_2 sorption isotherms for bilayer FG nanosheets.
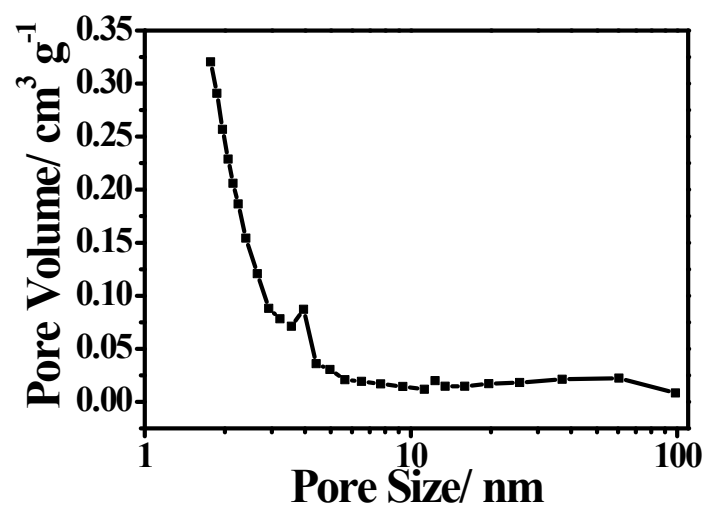
Figure S14. Pore size distribution of bilayer FG nanosheets.
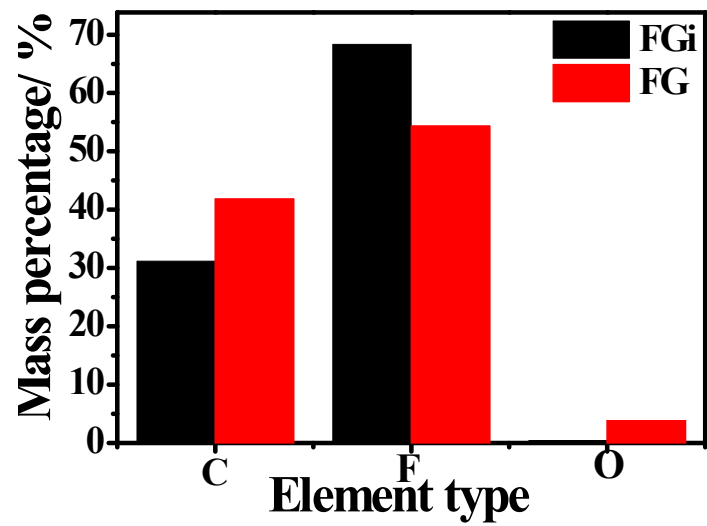
Figure S15. The detailed mass contents (C, O and F) of FGi and bilayer FG nanosheets.
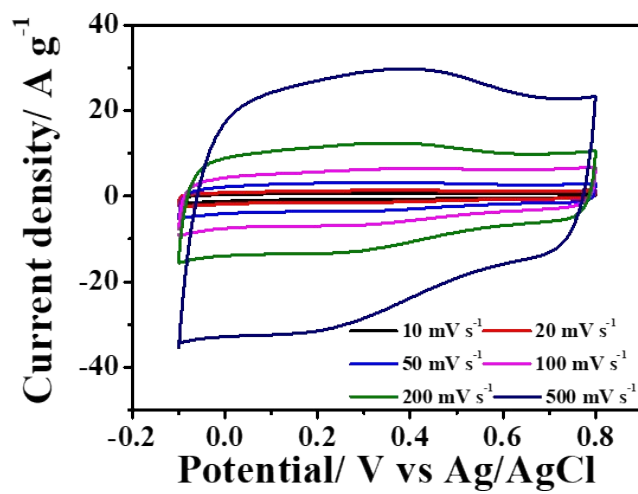
Figure S16. The CV curves of bilayer FG nanosheets as the scan rate was increased from 10 mV s^{-1} to 500 mV s^{-1}.
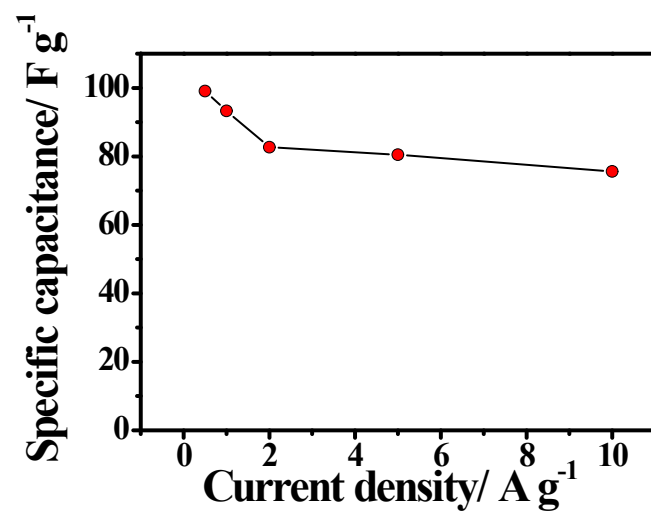
Figure S17. Rate-dependent specific capacitance of bilayer FG nanosheets electrode based supercapacitor when current densities increase from 0.5 to 10 A g^{-1}.
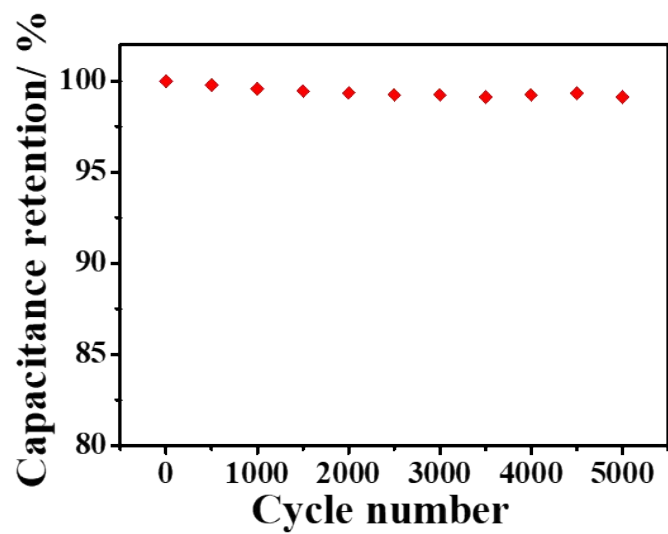
Figure S18. Cycling performance of bilayer FG nanosheets electrode based supercapacitor.
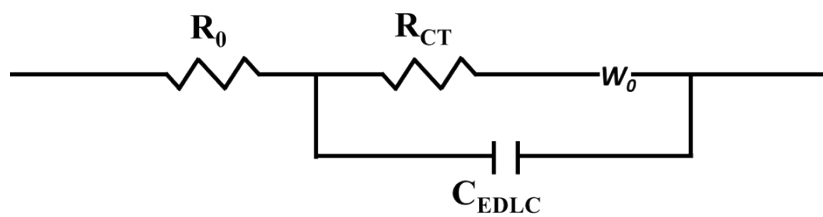
Figure S19. Equivalent circuit of bilayer FG nanosheets electrode and FGi electrode. Ro is the equivalent ohmic resistance, including resistance of the electrolyte and the internal resistance of the electrode. C_{EDLC} is electrical double-layer capacitance, *Wo* is the finite-length Warburg diffusion element, R_{CT} is charge transfer resistance.
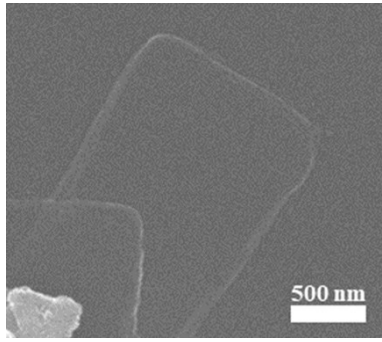
Figure S20. The SEM image of FG nanosheets after 20000 cycles.
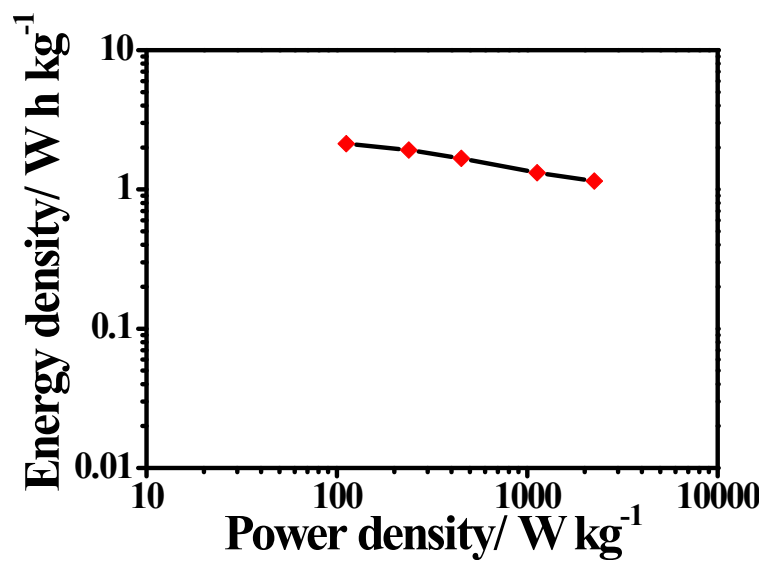
Figure S21. The Ragone plot of bilayer FG nanosheets electrode based solid-state supercapacitors.
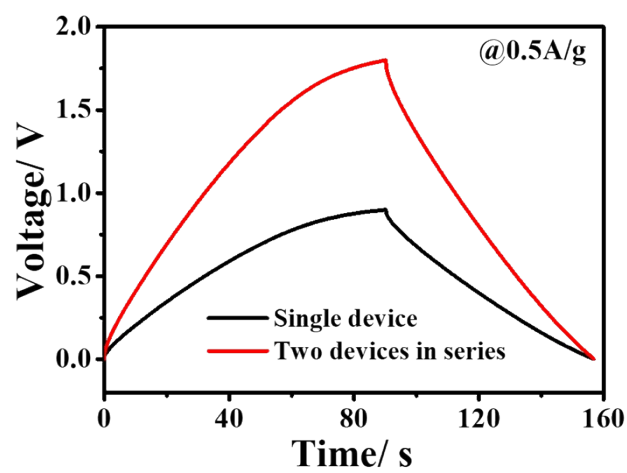
Figure S22. Galvanostatic charge and discharge curves of two solid-state supercapacitors in series at 0.5 A/g.
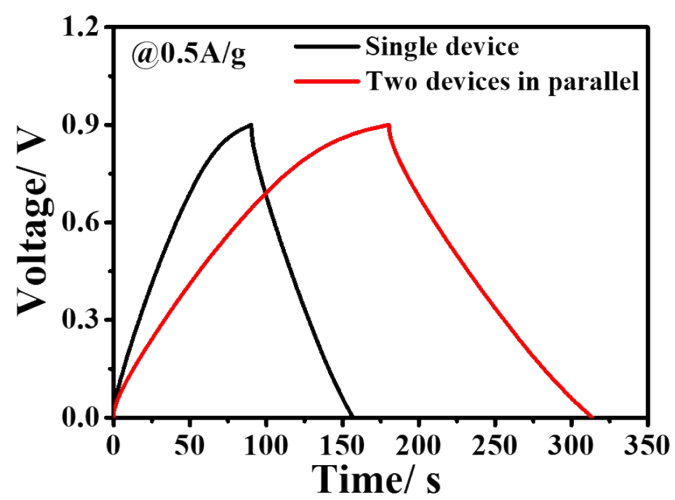
Figure S23. Galvanostatic charge and discharge curves of two solid-state supercapacitors in parallel at 0.5 A/g.

Supplementary Table.

Table S1. Comparison of exfoliation effect at different discharge current densities by a designed Li-ion battery.

Discharge current densities (mA g⁻¹)	Capacity (mAh g⁻¹)	Mass of FG nanosheets (g)	Thickness (nm)	Exfoliation efficiency (%)
10	311.0	0.269	~1.5	29.9
25	124.9	0.045	~1.5	5
50	20.1	Only particles	~180	0

Table S2. The bonding energy of each element and the detailed deconvolution of bilayer FG nanosheets and FGi.

Binding energy / Material	C=C (284.7 eV)	C-C-F (285.7 eV)	C-C-O (287.1 eV)	Covalent C-F (289.7 eV)	C-F$_2$ (291.4 eV)
bilayer FG nanosheets	21.2%	9.2%	10.4%	47.4%	11.8%
FGi	2.6%	—	—	65.4%	32.0%

Table S3. Comparison of the thickness and layer number of FG nanosheets from various exfoliation method.

Exfoliation method	Thickness (nm)	Layer number	Reference
sonication in ionic liquids	1-4	1-5	S1
sonication in 2-isopropanol	10	~12	18
grinding with Na_2O_2 and HSO_3Cl	4.7-15.5	5-16	S2
sonication in ethanol	2.57	3	S3
ball milling with KOH	4.6-5.7	4-7	S4
Hummers method using graphite fluoride	2.4 -2.8	3-4	S5
electrochemical-assisted sonication	1.5	2	This work

Supplementary References

S1.   H. Chang, J. Cheng, X. Liu, J. Gao, M. Li, J. Li, X. Tao, F. Ding and Z. Zheng, *Chem-Eur J*, 2011, **17**, 8896-8903.

S2.   Y. Yang, G. Lu, Y. Li, Z. Liu and X. Huang, *Acs Appl Mater Inter*, 2013, **5**, 13478-13483.

S3.   M. Zhang, Y. Ma, Y. Zhu, J. Che and Y. Xiao, *Carbon*, 2013, **63**, 149-156.

S4.   G. Zhang, K. Zhou, R. Xu, H. Chen, X. Ma, B. Zhang, Z. Chang and X. Sun, *Carbon*, 2016, **96**, 1022-1027.

S5.   W. Kang and S. Li, *Rsc Advances*, 2018, **8**, 23459-23467.